



Invited Review Article

Pb isotopes – A multi-function tool for assessing tectonothermal events and crust-mantle recycling at late Archaean convergent margins

J. Halla*

Natural Sciences Unit, Finnish Museum of Natural History, P.O. Box 44, FIN-00014, University of Helsinki, Finland

ARTICLE INFO

Article history:

Received 1 May 2018

Accepted 24 August 2018

Available online 5 September 2018

Keywords:

Pb isotopes

Archaean granitoids

Archaean plate tectonics

Convergent continental margins

Plate boundaries

Crustal recycling

Crustal isotope signature

Tectonothermal events

Secondary K-feldspar

Isochron

Paleoisochron

ABSTRACT

Lead isotopes are a powerful tool in studying Archaean granitoids and continental growth, because ^{207}Pb is a sensitive indicator of involvement of lead from old Archaean crustal sources. This paper aims to demonstrate the significance and promote the use of lead isotopes by reviewing the theory, concepts, and traditions for interpretations of Pb isotope data as well as by introducing a global model based on crust-mantle recycling for discriminating late Archaean convergent margin settings of granitoids. Case plots of K-feldspar and whole-rock data of ca. 2.7 Ga granitoids from several Archaean cratons show that lead isotope systematics, when interpreted in the correct geological context, can be used for resolving many questions on crustal evolution from magmatic and tectonothermal history of individual intrusions to large-scale tectonics and supercontinent correlations.

© 2018 Published by Elsevier B.V.

Contents

1.	Introduction	208
2.	Theory and concepts	208
2.1.	Pb isotopes	208
2.2.	μ , ω and κ	208
2.3.	Growth curves and isochrons	208
2.3.1.	Single-stage growth curve	208
2.3.2.	Pb–Pb isochron	209
2.3.3.	Two-stage growth curve	209
2.3.4.	Common lead	209
3.	Models and milestones	209
4.	Detecting tectonothermal events	211
4.1.	Low-grade metamorphism and secondary K-feldspar isochrons	211
4.2.	High-grade metamorphism and paleoisochrons	211
4.3.	U-loss and high Th/U trends	212
5.	Assessing convergent tectonic settings	213
5.1.	Recycling of lead at continental margins	213
5.2.	Time-fixed Pb recycling model for 2.7 Ga mantle-derived granitoids	213
5.2.1.	Model Pb isotope signatures in the mantle	213
5.2.2.	The model crust-mantle mixing line	213
5.2.3.	Model regression lines	213
6.	Case studies and discussion	215
6.1.	Crust-mantle recycling in the Superior and Slave provinces	215

* Corresponding author.

E-mail address: jaana.halla@helsinki.fi.

6.2.	The high-grade Limpopo belt, South Africa	215
6.2.1.	Extreme Eoarchaean Pb isotope sources	215
6.2.2.	High Th/U trends in high-grade metamorphic terrains	216
6.3.	Global Pb isotope pattern	216
6.3.1.	Convergent margins	216
6.3.2.	Convergent oceanic-oceanic boundaries	216
6.3.3.	Convergent continental margins	217
6.3.4.	Continental collisions	217
6.3.5.	Correlating ancient continental margins	218
6.3.6.	Granitoids and the growth of continents	218
6.4.	A case study from West Karelia Province, eastern Finland	218
6.5.	Concluding remarks	218
	Acknowledgements	220
	Appendix A. Equations describing the evolution of lead	220
	Appendix A. Supplementary data	220
	References	220

1. Introduction

The first measurements of lead isotopes were carried out in the early twentieth century by a newly invented device, the modern mass spectrometer (Aston, 1919; Dempster, 1917). The first measurement of the isotope composition of lead was carried out by Aston (1927). During the following decades, many scientists made important discoveries and models. There were two main avenues for early method development, 1) geochronology and 2) igneous rock and ore petrogenesis.

The first avenue led to the expansion of the most used rock-dating method today, the U–Th–Pb geochronology. For a full review of the historical development of the U–Pb zircon method, the reader is referred to Davis et al. (2003). The second avenue, which this article is all about, brought the tools for petrogenetic studies of igneous rocks and ores (for development and references, see section 3). The lead isotope geochemistry was popular from 70's to 90's, but declined at the turn of the millennium. The speculated reasons are the lack of model development, the attractiveness of the Lu–Hf method and modern in situ techniques, and the complexity of the interpretation of the Pb isotope systems.

The strength of the lead isotope method is in the existence of three decay series that produce radiogenic lead: $^{238}\text{U} \rightarrow ^{206}\text{Pb}$, $^{235}\text{U} \rightarrow ^{207}\text{Pb}$, and $^{232}\text{Th} \rightarrow ^{208}\text{Pb}$. The decay series support each other and give much more information for granitoid petrology than radiogenic isotopes based on a single parent–daughter pair. Decoupling of the parent isotopes U and Th in geological processes leaves traces in the lead evolution path that are possible to reveal by using appropriate assumptions, calculations and diagrams.

The strength brings also complexity; interpretation of lead isotope data is often a difficult task requiring appropriate lead evolution models and solid knowledge on the age, geochemistry, and the geological setting of the samples. However, careful interpretation in right geological context can give insights into several events in the history of a granitoid, such as crystallization, high-grade metamorphism, retrograde metamorphism, and crustal contribution.

Lead isotopes are a powerful tool in studying crustal recycling in the Archaean because of strong decoupling of U and Pb between crust and mantle and the shorter half-life of the ^{235}U isotope (parent to ^{207}Pb) compared with that of ^{238}U (parent to ^{206}Pb). Therefore, the abundance of ^{207}Pb increased more rapidly than that of ^{206}Pb , thus making the ^{207}Pb – ^{206}Pb pair a sensitive indicator of involvement of crustal lead.

This paper aims to demonstrate the significance and promote the use of lead isotopes by reviewing the theory and concepts, introducing several ways to interpret Pb isotope data, suggesting a global Pb–Pb pattern for Neoproterozoic supercontinent formation based on 2.7 Ga mantle-derived granitoids, and presenting and discussing case studies from different cratons.

2. Theory and concepts

2.1. Pb isotopes

Lead has four naturally occurring stable isotopes: nonradiogenic ^{204}Pb (used as index isotope) and the final decay products of three complex decay chains from uranium (U) and thorium (Th). ^{238}U and ^{235}U decay to ^{206}Pb and ^{207}Pb , respectively. Thorium exists primarily as one long-lived radioactive isotope, ^{232}Th , which decays to ^{208}Pb . Radioactive decay of uranium and thorium constantly changes the isotope composition of lead.

The lead isotope composition of a closed system, such as a mineral or a whole rock, depends on its initial Pb/Pb, U/Pb, and Th/Pb ratios. The Pb/Pb ratios of minerals vary widely from the highly radiogenic lead in very old U- and Th-rich minerals to the ‘common lead’ occurring in minerals that have very low U/Pb and Th/Pb ratios. The lead isotope composition of a rock or a mineral may change by decay of uranium and thorium as well as by mixing with lead from other sources.

2.2. μ , ω and κ

The evolution of lead in the Earth occurs in variable chemical environments (mantle, crust, and minerals enriched or depleted in U) having different U/Pb and Th/Pb ratios due to geochemical differentiation. The chemical environment, or chemical indexes, also termed milieu indexes, are described by Greek letters μ (Mu), ω (Omega) and κ (Kappa). These indexes simply refer to certain present-day isotope ratios of the system in which lead evolves. μ is the $^{238}\text{U}/^{204}\text{Pb}$, ω is the $^{232}\text{Th}/^{204}\text{Pb}$ and κ is the $^{232}\text{Th}/^{238}\text{U}$ ratio.

A high- μ rock, for example, contains much more U than Pb, and therefore, with time, develops a more radiogenic composition - provided that the system has remained closed since its formation. Respectively, a low- μ rock develops a less radiogenic composition. The μ , ω , and κ values can be calculated from measured Pb/Pb ratios and either U, Th, and Pb concentrations or initial Pb/Pb ratios and time (Eqs. (2) and (5) in Appendix A).

2.3. Growth curves and isochrons

2.3.1. Single-stage growth curve

A **growth curve** is a graph that describes the change of the Pb/Pb ratios with time. An uraniumogenic growth curve plots the constant change of the isotope ratios $^{207}\text{Pb}/^{204}\text{Pb}$ and $^{206}\text{Pb}/^{204}\text{Pb}$ due to the radioactive decay of uranium. Respectively, a thorogenic growth curve plots the change of the ratio $^{208}\text{Pb}/^{204}\text{Pb}$ with respect to $^{206}\text{Pb}/^{204}\text{Pb}$. The starting point of a growth curve in a closed system (e.g. in a whole rock sample) is called the **initial Pb isotope composition**.

The evolution path of lead on the uraniumogenic growth curve depends on the μ -value of the system. The initial lead isotope composition evolves along the growth curve through a series of time points, until the present-day isotope composition. The evolution of lead can be described on $^{207}\text{Pb}/^{204}\text{Pb}$ vs. $^{206}\text{Pb}/^{204}\text{Pb}$ or $^{208}\text{Pb}/^{204}\text{Pb}$ vs. $^{206}\text{Pb}/^{204}\text{Pb}$ diagrams in terms of growth curves based on Eqs. (1–5) in Appendix A.

Fig. 1 shows a plot of a single-stage growth curve on a $^{207}\text{Pb}/^{204}\text{Pb}$ – $^{206}\text{Pb}/^{204}\text{Pb}$ diagram. The curve rises steeply at first, because initially more ^{207}Pb than ^{206}Pb is produced, but then flattens as ^{235}U becomes depleted because it decays more rapidly than ^{238}U .

2.3.2. Pb–Pb isochron

For any suite of samples of the same rock outcrop having the same initial composition, there would be a family of growth curves because the samples have different μ -values (Fig. 2). Each sample follows the growth curve along a course designated by its μ -value. As the equation (Eqs. 6–8 in Appendix A) governing the growth curves is only a function of time, present-day samples of the same age but different μ -values plot along a straight line called an **isochron**. The slope of the isochron gives the age of the sample.

2.3.3. Two-stage growth curve

Growth curves can be calculated for different closed systems in which lead has evolved, for example for the source and the whole rock separated from the source. In Fig. 3, the lead started to evolve at t_1 in a source with a definite μ -value. After some time at t_2 , the lead moved into a crystallizing whole rock, and evolved in a new μ environment until the present-day. The present-day (t_0) lead isotope compositions of whole-rock samples with different μ -values plot on the whole-rock isochron, the slope of which gives the age of the rock. Also, multiple stages of growth in different μ environments can be easily calculated. The Pb/Pb ratios at the end of each system are calculated backward from present.

2.3.4. Common lead

The term **common lead** refers to Pb/Pb isotope ratios in a low-U and low-Th mineral, in which the production of radiogenic lead has been insignificant since its formation.

Lead on Earth consists of primordial lead that existed at the time of the formation of the Earth and radiogenic lead that formed by radioactive decay in U- and Th-bearing systems of Earth. At some point, lead may incorporate in a common-lead mineral that retains the same lead isotope composition since its formation. Examples of such minerals are galena (PbS) and K-feldspar (KAlSi₃O₈), in which Pb²⁺ replaces K⁺. Common lead in galena is used for evolution models and the study of ore deposits, and K-feldspar may provide the initial lead isotope compositions of granitoids.

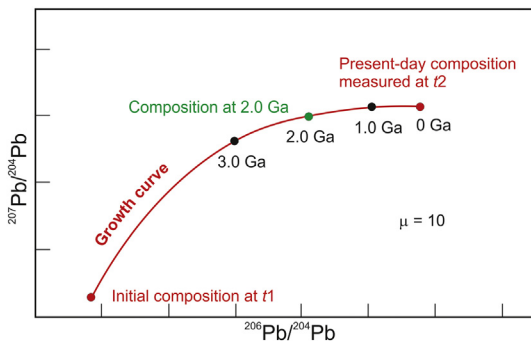


Fig. 1. Single-stage growth curve. The isotope ratios of Pb change along a growth curve from the initial composition at t_1 to the present-day composition at t_2 . The path of the growth curve depends on the μ -value of the system (10). The growth curve represents a sequence of points of times.

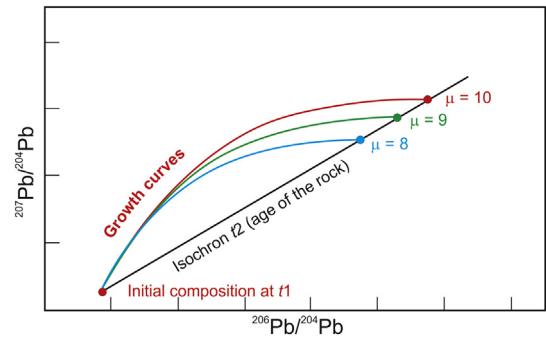


Fig. 2. Formation of the whole-rock isochron. Whole-rock samples with different μ -values evolve along different growth curves starting from the initial composition at the time of crystallization (t_1) to the present-day (t_2) whole-rock compositions. Whole-rock samples (circles) plot on a straight regression line, isochron, the slope of which gives the age of the rock. The age of the Earth was determined by this method.

To identify the source from which common lead originates, a model describing the evolution of the lead source is needed. With appropriate lead evolution models, the $^{207}\text{Pb}/^{204}\text{Pb}$ ratios in K-feldspars of Archaean granitoids should give information on a possible crustal component in their source.

3. Models and milestones

The history of common lead geology consists of many important discoveries. In 1938, Nier (1938) observed that lead ores have very variable isotope compositions likely related to mixing of radiogenic lead with primordial lead. This work led many scientists to hypothesize that the age of the Earth and the age of common lead minerals could be determined using quantitative models based on the isotopic evolution of lead in the Earth.

The first big milestone in the lead isotope research was the describing of the evolution of Earth's lead by a simple 'single-stage' model formulated independently by Holmes (1946) and Houtermans (1946) and was therefore termed as the **Holmes-Houtermans model** (Fig. 2). The model is based on several assumptions on a uniform Earth and closed regional U–Pb systems (for further explanation, see Halla, 2014). This model is referred to as a single-stage evolution model because lead has evolved in a single μ environment - i.e. the lead evolves along a single growth curve - before isolation from uranium to a common lead mineral.

The greatest achievement in the mid-century was finding out **the age of the Earth**. An age of 4.55 ± 0.07 billion years was achieved by Pb–Pb dating of several meteorites including the Canyon Diablo meteorite (Patterson, 1956) by using the Holmes-Houtermans method. This date is close to today's accepted age 4.54 ± 0.05 Ga.

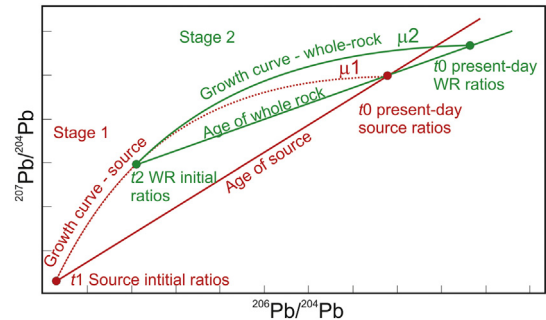


Fig. 3. Lead evolves from the initial composition at t_1 to the composition at t_2 along a growth curve μ_1 (stage 1, red). The μ -value changes at t_2 , and lead continues its evolution along another growth curve μ_2 (stage 2, green) until present day. The lines connecting the initial and present-day ratios are isochrons. Modified from Stacey and Kramers (1975). WR = whole rock.

However, it was soon realized that the common lead compositions that fit with the single-stage model, termed as ‘ordinary leads’, are quite rare (Kanasewich, 1968). The leads that do not fit in the single-stage model are classified as ‘anomalous’. The anomalous leads can give negative dates that lie in the future. The interpretation of anomalous lead isotope compositions have been discussed mathematically e.g. by Russell and Farquhar (1960), Kanasewich (1968), and Gale and Mussett (1973), who explain the existence of anomalous lead by mixing of ordinary lead with varying amounts of radiogenic lead derived from U- and Th-bearing sources. A later work of Kramers and Tolstikhin (1997) concludes that the anomalous lead may be attributed to rapid crustal growth during the Archaean and increasing recycling of continental crust in the Proterozoic. However, the modeling presented in this paper will show that the recycling of continental crust was an active process already around the 2.7 Ga crustal growth peak.

In the 70’s Stacey and Kramers (1975) added a second stage to the Holmes-Houtermans model to better accommodate the anomalous lead data (hereafter termed as the S&K model). According to the model, the evolution of lead started at 4.5 Ga with the isotope composition of Canyon Diablo troilites. At 3.7 Ga, the values of μ and ω changed due to geochemical differentiation and remained constant until the present day (Fig. 3). The Stacey and Kramers model has been widely used to assess the mantle and crustal contributions by determining the second-stage μ -values from K-feldspars and compared with the model crust ($\mu = 9.735$) and mantle ($\mu = 7.192$) values.

The Holmes-Houtermans as well as Stacey and Kramers terrestrial lead evolution models are based on fixed μ -value(s). However, in real Earth there is rather a continuous change in μ and κ values due to open-system behaviour of lead during magmatic, hydrothermal and metamorphic processes as well as weathering. Therefore, the igneous and metamorphic rocks reflect multi-stage evolution of lead. Lead may have evolved in different μ and ω environments for varying lengths of time or changed composition by mixing in geological processes. Among many attempts to improve Pb evolution models by taking account the open-system behaviour were the models of Cumming and

Richards (1975) and Gancarz and Wasserburg (1977), which were based on changing μ - and ω -values with time.

At the turn of the 80’s Doe and Zartman (1979) and Zartman and Doe (1981) approached the problem of changing μ and ω by combining the evolution of lead with plate tectonics and created a ‘plumbotectonic’ model (hereafter termed as the Z&D model). They distinguished three broad sources for lead: upper mantle, upper continental crust and lower continental crust, and an additional short-lived mixing reservoir termed orogene. Based on observational data (Doe and Rohrbough, 1977), they modeled the geochemical behavior of U, Th, and Pb among these reservoirs. They also estimated the average present-day concentrations of U, Th, and Pb in the sources. The model was later refined by Zartman and Haines (1988).

Fig. 4 illustrates the basic scheme of the plumbotectonic model based on recycling of material in plate tectonic processes. Orogenies occurring at 400 Ma intervals extracted U, Th, and Pb from the three sources (with a decreasing mantle contribution through time), mixed them in the orogene reservoir, and redistributed them back to the crustal and mantle sources.

The contributing crustal material comprises a vertically recycled component from the upper crust (erosional processes) and a horizontally recycled component (continental collapsing), representing the total crust. The low U/Pb ratio of the lower crust is due to the fractionation of uranium into the upper crust during granulite-facies metamorphism.

Fractionation of U, Th, and Pb to the upper crust and subsequent radioactive decay create distinct isotope characteristics of isolated sources that remain as closed systems between orogenies. Tectonic processes evenly spaced in time tend to reduce the isotopic differences by opening the closed systems and allowing mixing of the lead between different sources.

It seems that the Z&D model has not received as much attention as it should have, and generally, the S&K model has been favoured. However, there are two fundamental differences between the S&K and Z&D model. Firstly, the Z&D model takes account mixing in the plate tectonic

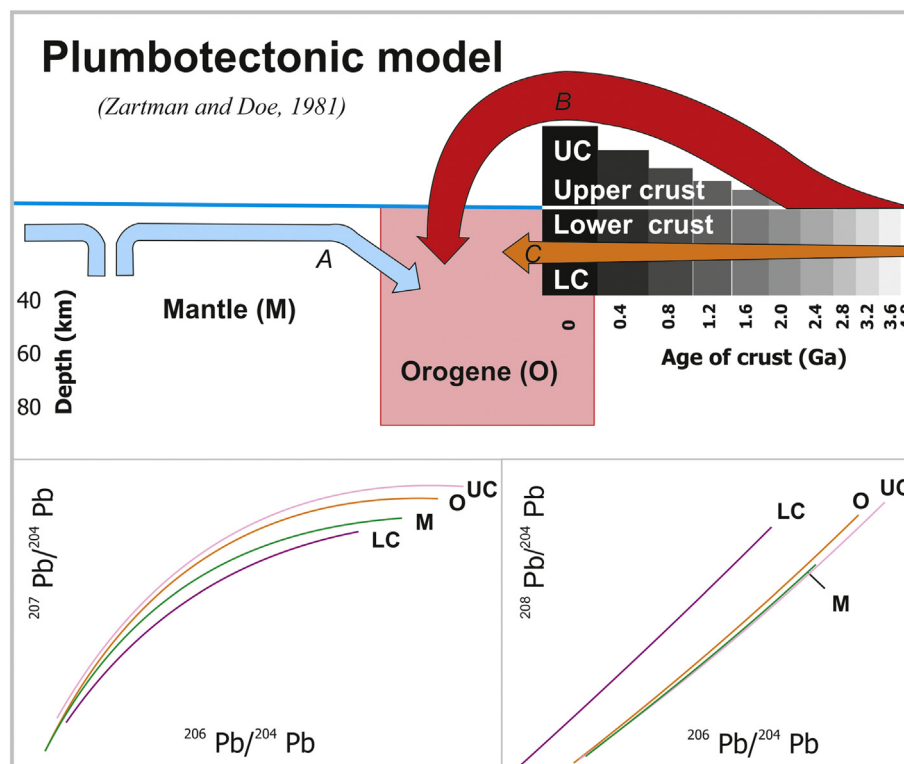


Fig. 4. The basic principles of the plumbotectonic model illustrating mixing of material from crustal and mantle reservoirs (A = mantle, B = upper crust, C = lower crust) into the orogene reservoir and the resulting Pb isotope evolution curves. Modified from Zartman and Doe (1981).

processes; instead of depending only on μ - or ω -values, the Z&D evolution model represents a series of lead isotope compositions (points of the evolution curve) that have formed at certain intervals by mixing of lead from different sources during orogenic processes. In other words, the time points of the Z&D model represent mixing of lead, whereas the S&K curves represent change only by radioactive decay. The calculations for the Z&D model values include also estimations of the concentrations of U, Th, and Pb at certain intervals. Secondly, the Z&D model is based on a large amount of real data (3458 analyses) from the Lead Isotope Data Bank of the U.S. Geological Survey (Doe and Roubough, 1977).

In summary, the previous research has led to wide variation of applications that are useful to metamorphic and igneous petrology as described in the next sections.

4. Detecting tectonothermal events

Tectonothermal effects, especially in complexly metamorphosed and deformed Archaean terrains, complicate the interpretation of lead isotope results on granitoids, but also provide valuable information that assists in understanding the whole evolution history of a rock.

Both low- and high-grade tectonothermal events can affect the evolutionary history of a rock after crystallization by redistributing lead within a closed whole-rock system or changing the μ -value of the whole rock. This section explores how the effects of tectonothermal events appear on Pb–Pb diagrams.

4.1. Low-grade metamorphism and secondary K-feldspar isochrons

Feldspars of igneous and metamorphic rocks contain abundant lead but negligible amounts of uranium and thorium. Hence, the lead isotope compositions of K-feldspars remain unchanged over long periods, preserving the Pb/Pb ratios that incorporated into the K-feldspar during crystallization. After crystallization, the Pb/Pb ratios of the whole rock increase, but the K-feldspars retain the initial composition.

Zartman (1965) pointed out that the K-feldspar-whole rock pairs can give the crystallization ages in ideal circumstances, but redistribution of lead during later tectonothermal events may change the lead isotope composition of feldspar. Rosholt et al. (1973) explained that the redistribution of lead might occur within a closed whole-rock system between the mineral phases.

The lead isotope compositions of different mineral phases may be homogenized and incorporated into K-feldspar during a later chemical equilibration of a whole-rock sample; K-feldspar then preserves this new composition as a record of the whole-rock lead isotope composition at the time of the tectonothermal event. If a complete equilibrium is not achieved, the lead isotope composition of the K-feldspar is heterogeneous as it may have an incomplete mixture of the Pb/Pb composition of the least and most radiogenic phases of the rock.

The $^{207}\text{Pb}/^{204}\text{Pb}$ – $^{206}\text{Pb}/^{204}\text{Pb}$ diagram in Fig. 5 illustrates a hypothetical example of the redistribution of lead in a whole-rock system during a tectonothermal event.

If the rock has remained a closed system since its crystallization, the lead isotope composition of analyzed feldspar samples fall on the same line termed a **secondary K-feldspar isochron**. If the age of the rock (t_1) is known, the time of the redistribution event (t_2) can be calculated from the slope of the secondary K-feldspar isochron ($m(t_1-t_2)$) using Eq. (7) in Appendix A.

The slope of the whole-rock isochron gives the age of the rock (Eq. (8) in Appendix A). Concordance of several isochron ages for K-feldspar-whole rock pairs and the secondary K-feldspar isochron age would favor interpretation as an age of metamorphism.

The secondary K-feldspar isochron is useful for calculations even if complete redistribution would have not occurred; the partially redistributed lead isotopic compositions plot on the K-feldspar isochron between the least and most radiogenic phases of the rock. However, in

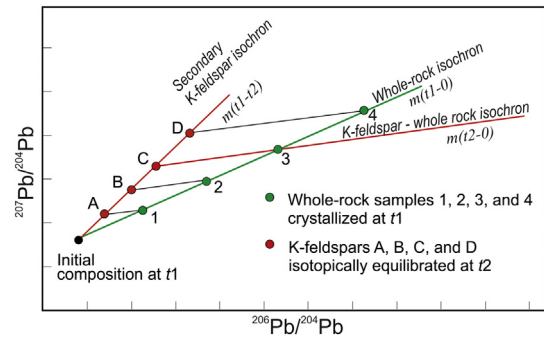


Fig. 5. A hypothetical example of the redistribution of whole-rock lead during a tectonothermal event, modified from Rosholt et al. (1973). The slope (m) of the secondary K-feldspar isochron represents the time elapsed from crystallization to the tectonothermal event (t_1-t_2), and the K-feldspar-whole rock isochrons represent the time elapsed from the tectonothermal event to present day (t_2-t_0).

this case, K-feldspar-whole rock pairs would not give a correct age. Partial redistribution of lead may occur at low-grade conditions, in which lead located in the crystal structures of accessory minerals does not participate the redistribution.

4.2. High-grade metamorphism and paleoisochrons

Several lead isotope studies confirm that many granulite-facies rocks show depletion in uranium relative to lower metamorphic grades. Dostal and Capedri (1975) found out that in amphibolite-facies rocks, most of the uranium is located along the grain boundaries, fractures, and cleavage planes of minerals as well as in accessory minerals, whereas in granulite-facies rocks the uranium is present almost exclusively in accessory minerals. They concluded that the fluids associated with dehydration during granulite-facies metamorphism washed away the uranium that was not located in accessory minerals or in crystal structures.

A comparatively short period between the crystallization of the rock and U-depletion in granulite-facies metamorphism probably does not have much effect on the whole-rock and K-feldspar isochron systems in a Pb–Pb diagram, but a substantial period may produce anomalous isochrons.

A classic example is provided by the Viken gneisses in Lofoten Vesterålen in NW Norway, which show an anomalous old whole-rock Pb–Pb isochron age, interpreted to result from the formation of the igneous protolith at 2.7–2.6 Ga, followed by a strong depletion in uranium at 1.8 Ga during granulite-facies metamorphism (Moorbath and Taylor, 1981).

Whole-rock Pb isotope ratios at the time of metamorphism define a line on a Pb–Pb diagram referred to as a **paleoisochron**. After depletion in uranium, the production of uranium ceases, and the present-day Pb isotope compositions fall on a line slightly transposed from the paleoisochron (Griffin et al., 1978). The slope of this **transposed paleoisochron** gives an anomalously high age.

Whitehouse (1989) investigated the effects of prograde amphibolite to granulite facies metamorphism on the Archaean Lewisian complex of north-west Scotland and observed that the Pb isotope homogenization either occurs or is incomplete or absent. He divided four different types of U–Pb behaviour during metamorphism. For further explanation, see Whitehouse (1989).

Halla et al., 2009 presented theoretical modeling on the effects of prograde (granulite facies) and later retrograde (amphibolite facies) metamorphism based on the concepts of a paleoisochron, transposed paleoisochron and secondary K-feldspar isochron (Fig. 6).

Model A (Fig. 6a) describes a situation in which the high-grade metamorphism occurred shortly after the formation of the rock at 2.73 Ga. The lead in a rock that experienced high-grade metamorphism (t_2) shortly after crystallization (t_1). The time gap t_1-t_2 has no effect on

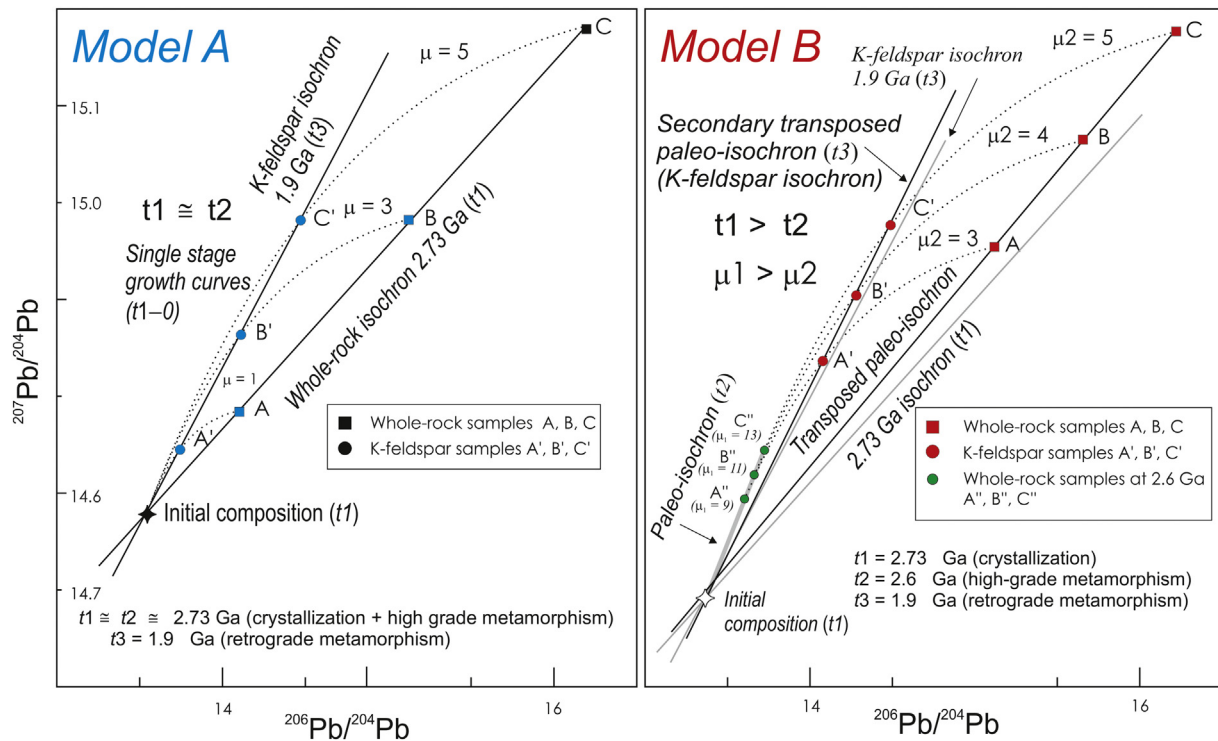


Fig. 6. a) Model A describes the evolution of lead in a rock that experienced high-grade metamorphism (t_2) shortly after crystallization (t_1) and later underwent retrograde metamorphism (t_3). b) Model B represents the evolution of lead in a rock that experienced high-grade metamorphism (t_2) 130 Ma after crystallization (t_1), and later underwent retrograde metamorphism (t_3).

the whole-rock isochron. The present-day whole-rock samples A, B, and C with μ values of 1, 3, and 5 yield a whole-rock isochron age of 2.7 Ga representing the igneous crystallization age t_1 .

Owing to complete redistribution of lead during retrograde metamorphism, the present-day K-feldspar samples A', B', and C' represent the lead isotope composition of the whole-rock samples A, B, and C at 1.9 Ga (t_3), defining a K-feldspar isochron equivalent to the whole-rock paleoisochron (2.73 Ga at 1.9 Ga).

The time of metamorphism can be calculated from the slope of the K-feldspar isochron (Eq. (7) in Appendix A). The whole-rock isochron and the K-feldspar isochron intersect at a point representing the initial composition of the lead at 2.7 Ga (t_1).

Model B (Fig. 6b) involves a protolith with higher μ ($^{238}\text{U}/^{204}\text{Pb}$) values between the formation at 2.73 Ga and the high-grade metamorphism at 2.6 Ga. During this period, the protolith of Model A developed more radiogenic lead isotopic compositions than the protolith of Model B. The evolution of lead occurred in a rock that experienced high-grade metamorphism 130 Ma after crystallization. In this case, the time gap between crystallization and high-grade metamorphism (t_1 - t_2) has a detectable effect on the present-day lead isotope compositions.

The rock crystallized at 2.7 Ga (t_1). The lead evolved in an environment with μ -values of 9, 11, and 13 (μ_1) between t_1 and t_2 , resulting in whole-rock compositions A'', B'', and C'' by 2.6 Ga (t_2). High-grade metamorphism at 2.6 Ga (t_2) gave rise to significantly lower μ -values of 3, 4, and 5 (μ_2) until present day (t_2 - t_0).

Owing to complete redistribution of lead during retrograde metamorphism at 1.9 Ga (t_3), present-day K-feldspar samples A', B', and C' represent the lead isotope composition of the whole-rock samples A, B, and C at 1.9 Ga (t_3). The K-feldspar isochron is slightly transposed from the 1.9 Ga whole-rock paleoisochron (gray line) owing to the change in μ value at 2.6 Ga. The term **secondary transposed paleoisochron** is applied to the observed K-feldspar isochron.

The present-day whole-rock samples fall on a transposed paleoisochron, which is slightly disposed from the whole-rock isochron

indicated by a gray line. In this case, the whole-rock isochron gives an anomalous old age.

As an implication of the time gap between crystallization and granulite-facies metamorphism on the Pb–Pb diagrams, a gap forms between the initial and the least radiogenic lead isotope compositions of whole-rocks (A) or K-feldspar (A') (Fig. 6). Consequently, the K-feldspar does not represent the initial composition of the granitoid. A time gap between crystallization and metamorphism may lead to more radiogenic apparent initial Pb isotope compositions and anomalously high whole-rock isochron ages.

4.3. U-loss and high Th/U trends

High-grade metamorphic rocks show often depletion of uranium relative to thorium. Keppler and Wyllie (1990) suggested that interactions with CO_2 -bearing fluids could account for the high Th/U ratio, because only uranium forms complexes with chloride or CO_2 . Lead seems to be rather immobile during granulite-facies conditions. High Th/U ratio of a granitoid formed when U and Th escaped from the crystal structures in granulite-facies metamorphism. Subsequently, CO_2 -bearing fluids washed away the U located along the grain boundaries, while Th remained, generating the high Th/U ratios of the rock.

To explore the effects of lowered U and elevated Th/U ratios in whole-rock systems, Fig. 7 shows two hypothetical sets of 2.7 Ga whole rocks with different ranges of μ -values (but the same range of ω -values).

The plots on the $^{207}\text{Pb}/^{204}\text{Pb}$ – $^{206}\text{Pb}/^{204}\text{Pb}$ diagrams present calculations from hypothetical initial compositions with two sets of μ -values: 1–20 describing rocks that are not depleted in U, and b) 1–5 describing a U loss of 75% at the time of formation. In Fig. 7a) the set with lower μ -values plot relatively close to the initial compositions compared with the set with higher μ -values. A $^{208}\text{Pb}/^{204}\text{Pb}$ – $^{206}\text{Pb}/^{204}\text{Pb}$ diagram in Fig. 7b) shows that a 75% loss of U changes the κ value significantly. The average Stacey and Kramers (1975) κ value is 3.78, whereas many Archaean rocks show κ values as high as 15.

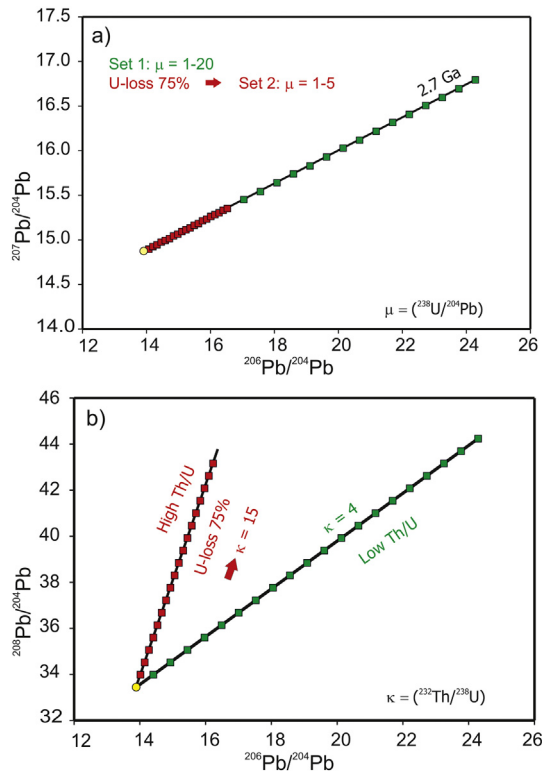


Fig. 7. Hypothetical (a) $^{207}\text{Pb}/^{204}\text{Pb}$ – $^{206}\text{Pb}/^{204}\text{Pb}$ and (b) $^{208}\text{Pb}/^{204}\text{Pb}$ – $^{206}\text{Pb}/^{204}\text{Pb}$ plots calculated for two sets of μ -values, 1–20 (green symbols) and 1–5 (red symbols), the latter describing a U loss of 75%.

5. Assessing convergent tectonic settings

5.1. Recycling of lead at continental margins

Continental crust is recycling at convergent plate boundaries; material from the continents erodes away, transfers into the mantle by subduction and possibly returns to the crust by magmatism (Fig. 8). There are two types of tectonic erosion; frontal erosion at the outer margin and basal at the base of the continental margin. By crustal recycling processes, radiogenic lead isotope signatures developed in different parts of the crust may enter the mantle and overprint the mantle composition. Identification of such crustal signatures in the mantle (and excluding other explanations), can be regarded as a proof of crustal recycling and subduction processes.

Lead that evolves in a high- μ system (e.g. U-enriched upper crust) develops a more radiogenic Pb isotope signature. Respectively, Pb evolved in an isolated low- μ system (e.g. old U-depleted lower crust) carries less-radiogenic Pb isotope signatures. If an old recycled high- or low- ^{207}Pb signature exists in the mantle, it may be inherited by mantle-derived rocks.

According to the current knowledge, Neoproterozoic continents formed by accretion of island arcs and oceanic plateaus around Mesoproterozoic microcontinents. By 2.7 Ga, the continental margins represented collages of crustal segments of different age; ranging from the oldest rocks at 4.0 Ga to juvenile 2.7 Ga rocks (Fig. 9).

Lead recycled from crustal segments of different ages can mix and overprint the mantle isotope compositions. Granitoids originating from this contaminated mantle may thus inherit isotope compositions that reflect the age of the continental margin at which they were generated. The isotope composition of lead recycling from the continental sources to the mantle depends on the age and U/Pb ratio of the source as well as on the amount of recycled Pb. In the Archaean, the amount of ^{207}Pb increased rapidly with respect to ^{206}Pb , which is a sensitive

indicator of involvement of lead evolved in very old long-lived crustal sources.

5.2. Time-fixed Pb recycling model for 2.7 Ga mantle-derived granitoids

Following the idea of plumbotectonics (Zartman and Doe, 1981), Halla (2014) suggested a time-fixed model for mantle-derived granitoids that were generated during the peak period of crustal growth at 2.7 Ga (Fig. 10). The model is based on the idea of recycling of lead from old continental margins into the subduction zone and emerging as inherited crustal signatures in newly-formed granitoids derived from this isotopically contaminated mantle. The model is termed hereafter as the 2.7 Ga Recycling Model (RM 2.7), since the diverse isotope signatures in the mantle (= model initial isotope compositions of granitoids) are the result of recycling and mixing of continental material into the mantle. The plotting parameters for the model are given in Table 1 (model isotope signatures in the mantle source = initial isotope compositions of granitoids) and Supplementary Table (model regression lines = whole-rock isochrons).

5.2.1. Model Pb isotope signatures in the mantle

Fig. 9 shows examples of hypothetical Neoproterozoic convergent margins at 2.7 Ga. Recycling of lead from crustal segments of different ages generates distinct crustal isotope signatures in the mantle.

A primitive oceanic island arc at an oceanic-oceanic boundary generated from a **Depleted Mantle (DM)** source does not show any signs of pre-existing crust (Fig. 9a). A more mature **Oceanic Island Arc (OIA)** of relatively newly formed crust at an oceanic-arc boundary created a mantle source with a slightly more radiogenic OIA-signature (Fig. 9b). Accretion of island arcs and < 3.2 Ga microcontinents at oceanic-continent boundaries produced a relatively **Young Continental Margin (YCM)** with a more radiogenic crustal signature (Fig. 9c). At continental boundaries, accretion of continents with segments older than 3.2 Ga created an **Old Continental Margin (OCM)** setting at which lead from upper crust (**OCM-UC**) or lower crust (**OCM-LC**) recycled to the mantle (Fig. 9d). Table 1 gives the Pb/Pb ratios and references for the selected model isotope signatures in the mantle source.

Old continental margins can have two strikingly contrasting lead sources, since the older upper crust (>3.2 Ga) had more time to produce radiogenic lead than the younger upper crust (<3.2 Ga). Consequently, the old high- μ upper crust may produce very radiogenic isotope compositions, whereas the low- μ lower crust that has been isolated from U for a long time retains very low radiogenic lead character. The high- μ crust can be produced by recycling of sediments from an old upper crust source, whereas the exposure of a low- μ crust might require more vigorous processes of continental collisions and erosion or delamination of lower crust. The extreme $^{207}\text{Pb}/^{204}\text{Pb}$ signatures may ultimately derive from Hadean protocrust (Kamber et al., 2003).

Young continental margins had less time to develop radiogenic differences between upper and lower crust, therefore these sources are not separated in the model.

5.2.2. The model crust-mantle mixing line

Mixing and homogenization of older crust-derived lead with the mantle on a regional scale results in a linear array in a $^{207}\text{Pb}/^{204}\text{Pb}$ – $^{206}\text{Pb}/^{204}\text{Pb}$ diagram, termed a crust-mantle mixing line. The mixing line is defined by the five model mantle signatures; DM, OIA, YCM, OCM-UC and OCM-LC (Fig. 9), also representing the model initial compositions for granitoids. Table 1 gives the model Pb isotope ratios and references for the signatures.

5.2.3. Model regression lines

Fig. 10 shows five regression lines (reference isochrons) calculated for hypothetical whole-rock systems with a slope of 2.7 Ga, starting from the respective five model end-member signatures representing the model initial compositions of the whole-rock systems (plotting

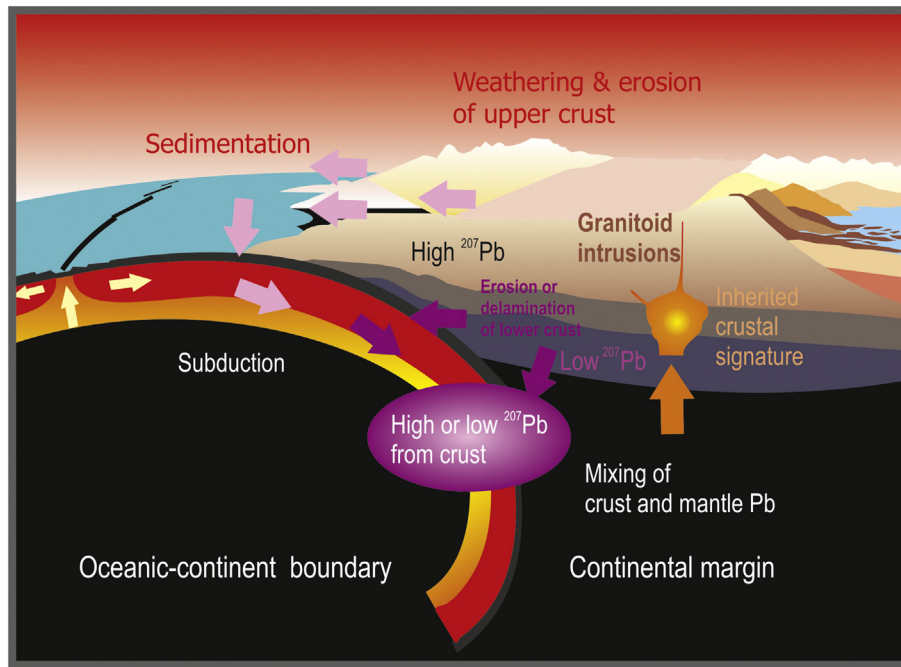


Fig. 8. A cartoon illustrating recycling of lead at a convergent continental margin. Lead isotope signatures generated in the crust recycle into the mantle by subducting sediments, mix and return to the crust with mantle-derived granitoid intrusions.

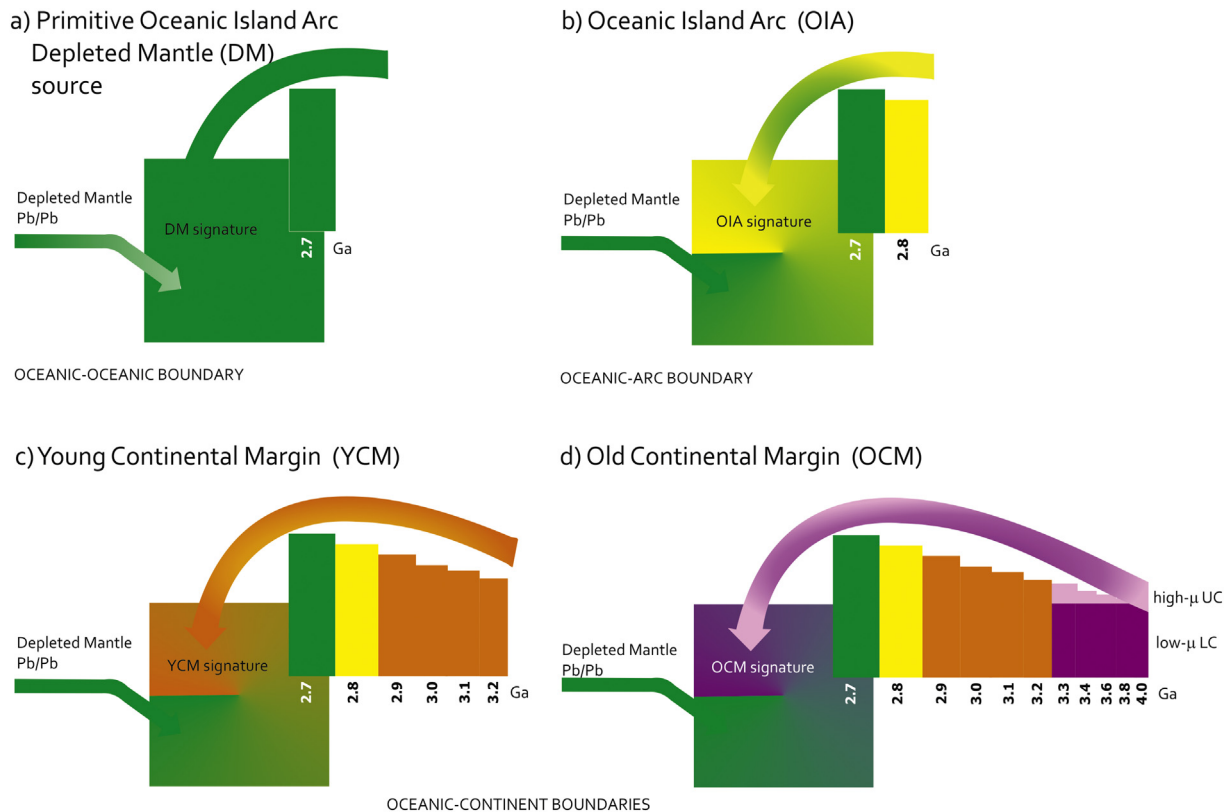


Fig. 9. Schematic drawings of hypothetical convergent margins at 2.7 Ga. The crustal isotope signatures in the mantle at plate boundaries are termed according to the age and nature of arc systems or continents from which the signatures were recycled. (a) Primitive Oceanic Island Arc with a Depleted Mantle (DM) source at an oceanic-oceanic boundary, (b) a more mature Oceanic Island Arc (OIA) of relatively newly formed crust (2.8–2.7 Ga) at an oceanic-arc boundary. (c) Young Continental Margin (YCM) including segments of <3.2 Ga crust at oceanic-continent boundary, and (d) Old Continental Margin (OCM) including segments of >3.2 Ga crust. The upper (UC) and lower (LC) OCM segments may carry very high- or low- radiogenic signatures depending on their U/Pb ratio and age.

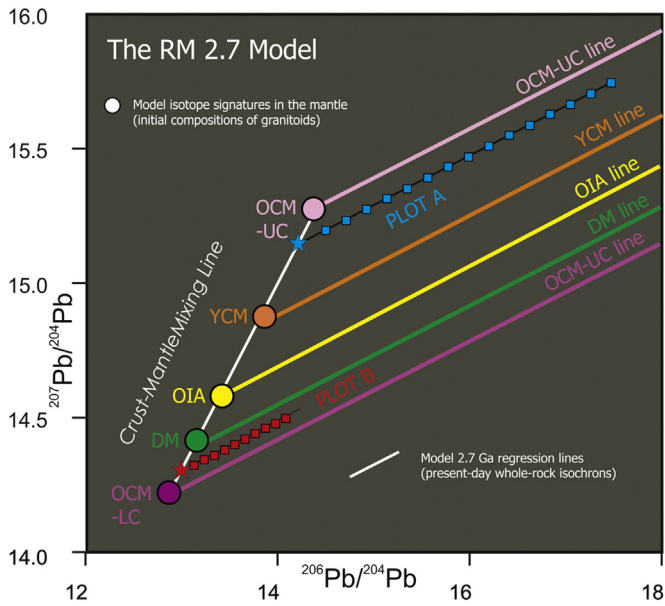


Fig. 10. The RM 2.7 model of Halla (2014) for mantle-derived granitoids. The line drawn through the model isotope signatures in the mantle forms a mantle-crust mixing line. The respective model reference lines represent 2.7 Ga whole-rock isochrons. Hypothetical plots of K-feldspars (stars) and whole rocks (squares) indicate old continental margin settings. Plot A indicates a high- μ upper crust source, whereas plot B suggests a contribution from a low- μ lower crust source. See Fig. 9 for acronyms.

parameters in Supplementary Table). The regression lines are termed respectively as DM, OIA, YCM, OCM-UC, and OCM-LC lines (see Fig. 9 for acronyms). The initial compositions and respective reference lines describe the age and nature of the tectonic environment of the granitoid.

For example, K-feldspars of a 2.7 Ga granitoid from a source contaminated by Eo- to Paleoarchean upper crust (>3.2 Ga) would plot close to the OCM-UC signature on the crust-mantle mixing line. The whole rocks would plot close and parallel to the 2.7 Ga OCM-UC line (Plot A in Fig. 10). If the source was contaminated by >3.2 Ga lower crust, K-feldspars would plot close to the OCM-LC signature and whole rocks parallel to the OCM-LC line (Plot B in Fig. 10). A 2.7 Ga mantle-derived granitoid may incorporate an initial Pb isotope composition of any mixture on the 2.7 Ga crust-mantle mixing line.

The benefit of the RM 2.7 model is that the intersection of a whole-rock isochron and the crust-mantle mixing line gives an estimation of the initial composition of the rock; the diagram is useful also for whole rocks without K-feldspar data. Especially the diagram helps to recognize sources of old crustal lead, even if later processes would have destroyed the old crust. The time-fixed model is also easy to recalculate to explore other significant peaks of crustal growth in Earth's history.

6. Case studies and discussion

This section explores case studies on the previously introduced diagrams designed to resolve problems on crust-mantle interactions at

convergent margins, identification of ancient collision zones, correlating Archaean cratons and, within intrusion level, to study tectonothermal effects after crystallization. The data used for the plots is presented in Supplementary Table.

6.1. Crust-mantle recycling in the Superior and Slave provinces

Classical examples of crust-mantle mixing arrays on Pb–Pb diagrams are the **Superior and Slave Arrays** formed by K-feldspars of 2.7 ± 0.1 Ga granitoids from the Canadian Shield (Davis et al., 1996).

In the RM 2.7 diagram (Fig. 11), the Superior K-feldspars (Ayer and Dostal, 2000; Carignan et al., 1993, 1995; Gariépy and Allégre, 1985; Henry et al., 1998; Isnard and Gariépy, 2004; Stevenson et al., 1999) plot on the model DM-YCM mixing line, between depleted mantle and young continental margin signatures. The RM 2.7 plot is consistent with the previous interpretations suggesting an evolution of oceanic island arc -type subduction zone, reflected by the low-radiogenic end of the array, into a young continental convergent margin, represented by the radiogenic end of the array. The RM 2.7 plot is consistent with the known history of the Superior Province; amalgamation between 2.72 and 2.68 Ga by accretion of juvenile island arcs with minor <3.2 Ga fragments.

K-feldspars of 2.7 ± 0.1 Ga granitoids from the Slave Province (Davis et al., 1996; Yamashita et al., 1999) plot on the YCM-OCM-UC model mixing line, between young continental margin and old continental margin upper crust signatures, suggesting an accretion of oceanic island arcs to a nucleus of very old upper crust. The RM 2.7 diagram is consistent with the age of the Slave Province; the western part of the province consists of rocks older than 3.2 Ga, including the oldest rocks in the world, the 4.0 Ga Acasta gneisses.

The Superior and Slave K-feldspar Arrays plotting on the RM 2.7 crust-mantle mixing line are consistent with rapid recycling of crustal material through subduction processes at Neoproterozoic continental margins that developed around Eo- to Mesoarchean nuclei.

6.2. The high-grade Limpopo belt, South Africa

6.2.1. Extreme Eoarchean Pb isotope sources

The Limpopo Belt is a high-grade metamorphic province, which consists of Archaean to Paleoproterozoic rock units and is bounded by granitoid-greenstone terrains of the Zimbabwe craton in the north and Kaapvaal craton in the south. The Limpopo Belt consists of three distinct domains separated by major shear zones: Central Zone, North Marginal Zone (NMZ) and South Marginal Zone (SMZ).

The RM 2.7 diagram in Fig. 12 shows striking differences in the isotope compositions of 2.7 ± 0.1 Ga granitoids from the northern and southern Limpopo belts as well as from the Kaapvaal and Zimbabwe cratons (Barton et al., 1992; Berger and Rollinson, 1997; Jelsma et al., 1996; Kreissig et al., 2000).

The whole rocks from the Limpopo NMZ show a trend following the model OCM-UC line, whereas data from the SMZ, together with the Kaapvaal data, cluster close to the initial compositions of the OCM-LC and DM lines. These contrasting trends indicate an old convergent continental margin setting, the former suggesting contributions from very old segments of high- μ upper crust and the latter from low- μ lower

Table 1
The RM 2.7 model initial Pb/Pb ratios (i.e. crustal signatures in the mantle^a).

Symbol color	Crustal signature	²⁰⁷ Pb– ²⁰⁴ Pb	²⁰⁶ Pb– ²⁰⁴ Pb	²⁰⁸ Pb– ²⁰⁴ Pb	Reference	Source of the lead
	DM	13.33	14.42	n.d.	Carignan et al. (1995)	Primitive island arc
	OIA	13.42	14.58	33.17	Zartman and Doe (1981)	Mature island arc
	YCM	13.90	14.87	33.52	Zartman and Doe (1981)	Island arcs and continental nuclei up to 3.2 Ga
	OCM-UC	14.36	15.27	34.26	Davis et al. (1996)	High- μ protocontinent 3.2–4.0 Ga
	OCM-LC	12.87	14.22	33.23	Zartman and Doe (1981)	Low- μ protocontinent 3.2–4.0 Ga

^a Explanation in Fig. 10.

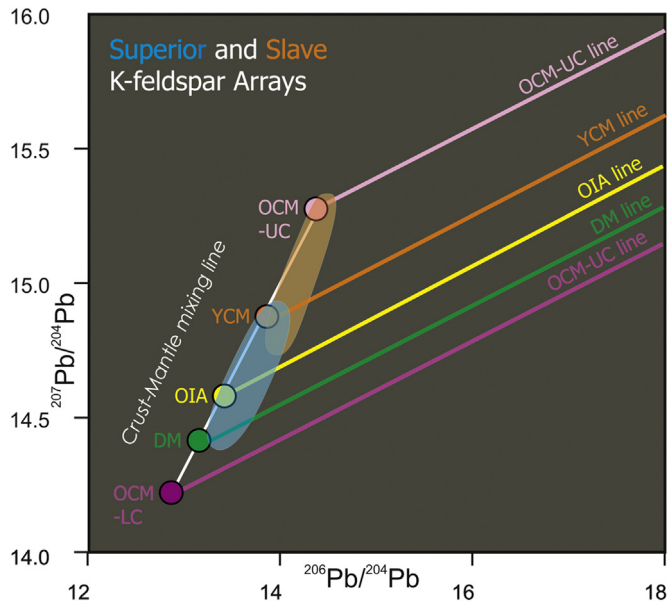


Fig. 11. Pb isotope compositions of K-feldspars in 2.7 ± 0.1 Ga granitoids from the northwestern Canadian Shield form distinct arrays on the crust-mantle mixing line of the RM 2.7 diagram, the Superior Array (blue field) and the Slave Array (orange field). See Fig. 9 for acronyms. Data and references in Supplementary Table.

crust. The Kaapvaal plot is consistent with the known age of the craton (3.7–2.7 Ga).

Granitoids from the Zimbabwe craton plot slightly above the YCM model line indicating the presence of high- μ crust slightly older than 3.2 Ga. This is consistent with the known age of the Zimbabwe craton (up to 3.5 Ga).

Globally, the most extreme radiogenic lead isotope compositions are found in the western Slave Province, Canada, and in the northern Limpopo belt in South Africa. The least radiogenic compositions are found in the southern Limpopo belt and some other cratons. The extreme isotope compositions of the Limpopo belt suggest contributions from Eoarchaean U-enriched upper crust or U-depleted lower crust, which was exposed for frontal and basal erosion during the collision of Kaapvaal and Zimbabwe cratons at 2.7 Ga.

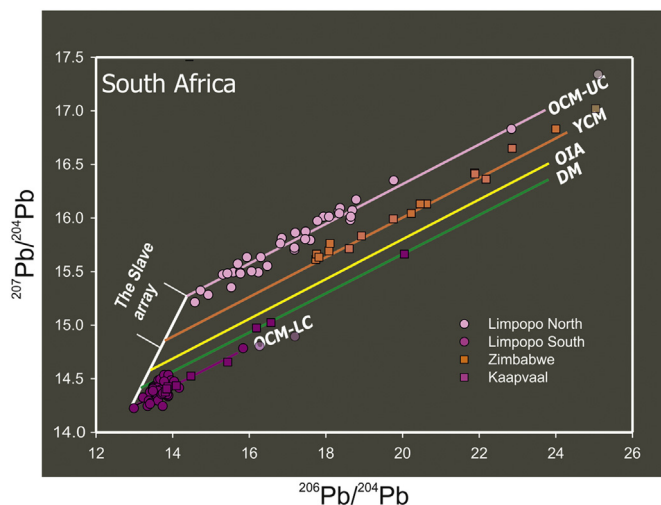


Fig. 12. Pb isotope ratios of 2.7 ± 0.1 Ga whole-rock granitoids from the northern and southern margins of the Limpopo belt as well as from the Kaapvaal and Zimbabwe cratons in South Africa plotted on the RM 2.7 diagram. See Fig. 9 for acronyms. Data and references in Supplementary Table.

6.2.2. High Th/U trends in high-grade metamorphic terrains

Long-time enrichment of a rock in Th over U generates distinct isotope compositions with high ^{208}Pb with respect to ^{206}Pb . Fig. 13 shows that highly metamorphic terrains of the Limpopo belt show very high Th/U trends with κ -values (present-day $^{232}\text{Th}/^{238}\text{U}$) up to 15, whereas lower metamorphic terrains of the Zimbabwe craton have retained their “average” Th/U ratio with κ -values around 4 (the average of Stacey and Kramers, 1975, is 3.78). High Th/U trends on diagrams with $\kappa = 15$ suggest that the rocks have lost about 75% of their uranium approximately at the time of crystallization (Fig. 7b).

The high Th/U trend of the Limpopo belt seems to be a consequence of the collision of the Kaapvaal and Zimbabwe cratons at 2.7 Ga. The identification of high and low Th/U trends of granitoids helps in recognizing high-grade terrains and, consequently, locating the ancient collisional zones.

6.3. Global Pb isotope pattern

6.3.1. Convergent margins

The RM 2.7 diagram for 2.7 Ga mantle-derived granitoids from different cratons (Fig. 14) presented in Fig. 15 is a summary diagram for whole-rock plots based on a compiled TIMS Pb isotope dataset of ca. 500 samples of 2.7 ± 0.1 Ga feldspars and granitoids from different cratons (data and references in Supplementary Table; individual plots in Halla, 2014). The diagram shows a clear pattern that describes the evolution of convergent margins from oceanic to continental at around 2.7 Ga.

6.3.2. Convergent oceanic-oceanic boundaries

Oceanic island arcs occur at convergent oceanic-oceanic boundaries. Their depleted mantle sources do not show any sign of crustal signatures; recycling of young crustal material during accretion of primitive island arcs or oceanic plateaus does not affect the mantle lead isotope compositions, because there is not enough time for radiogenic compositions to develop. In the RM 2.7 diagram, present-day Pb isotope compositions of K-feldspars of granitoids from oceanic island arcs plot on the mixing line close to the DM initial signature, and present-day whole-rock isochrons close and parallel to the respective DM line. The low-radiogenic end of the Superior K-feldspar Array reflects this stage.

Neymark et al. (1993) studied 3.0 Ga TTG granitoids from the Olekma granite-greenstone terrain of the Aldan Shield, eastern Siberia.

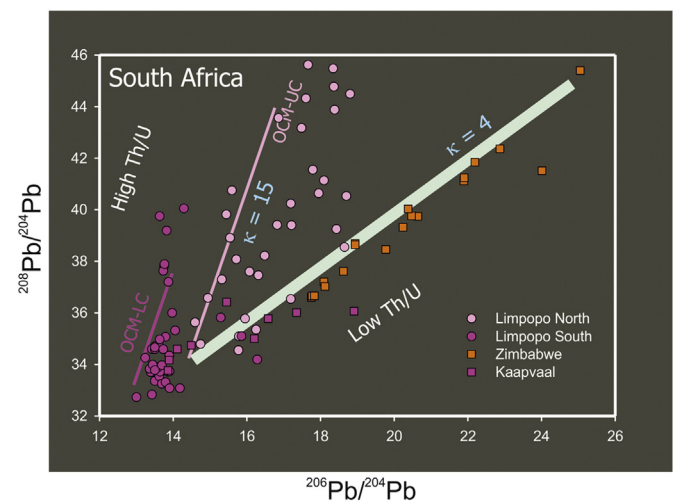


Fig. 13. 2.7 ± 0.1 Ga whole-rock granitoids from the high-grade metamorphic terrains of the Limpopo belt and lower-grade terrains of the Zimbabwe craton plotted on the $^{208}\text{Pb}/^{204}\text{Pb}$ vs $^{206}\text{Pb}/^{204}\text{Pb}$ diagram with the RM 2.7 model lines calculated for $\kappa = 15$ and $\kappa = 4$. See Fig. 9 for acronyms. Data and references in Supplementary Table.



Fig. 14. Major Archean cratons and provinces. Modified from Bleeker (2003).

They found no evidence of recycled crustal material, which indicates derivation from a depleted source. Fig. 15 shows that the data from the Olekma terrain plots close to the OIA line (note a slightly deeper slope because of older age) of the RM 2.7 diagram indicating a primitive oceanic island arc tectonic setting consistent with the previous interpretation.

6.3.3. Convergent continental margins

Progressive recycling of crustal sediments generated a more mature island arc setting (OIA) with a more radiogenic mantle wedge source showing an OIA signature. Maturing oceanic island arcs and

Mesoarchaean (<3.2 Ga) continental nuclei were assembled resulting in young continental margins (YCM) of relatively newly accreted crust. Because of increasing crust-mantle interactions, more radiogenic mantle sources were developed. In the RM 2.7 diagram, present-day Pb isotope compositions of K-feldspars plot on the mixing line between the DM and YCM initial compositions, and present-day whole-rock isochrons plot accordingly between the DM and YCM lines.

Data from West Karelian (Halla, 2005; Heilimo et al., 2013) and Grenville (Dickin, 1998; Gariépy et al., 1990) provinces show similar whole-rock isotope characteristics plotting between OIA and YCM lines. The results from West Karelian granitoids in eastern Finland are consistent with their suggested origin in an enriched mantle wedge below a mature island arc or young continental margin and the known age of the craton (2.8–2.7 Ga, with <3.2 Ga fragments).

Granitoid rocks from the Yilgarn (Bickle et al., 1983; McNaughton and Bickle, 1987; Oversby, 1975) and Zimbabwe (Jelsma et al., 1996) cratons as well as the more radiogenic end of the Superior Array show young continental margin trends. This is consistent with the known ages of the cratons ranging up to 3.3 Ga (Yilgarn), 3.5 Ga (Zimbabwe), and 3.2 Ga (Superior).

The Wyoming craton in North America (Rosholt et al., 1973; Wooden and Mueller, 1988) and Pilbara craton in Western Australia (Oversby, 1975) are known to include Paleoproterozoic fragments up to 3.6 Ga, which is consistent with the RM 2.7 model indicating the presence of an upper crustal segment older than 3.2 Ga. Wooden and Mueller (1998) attributed the crustal signature of 2.74–2.79 Ga mantle-derived granitoids from Wyoming to subduction of continental sediments from older high-μ crustal source and contamination of the overlying mantle wedge. These are consistent with the RM 2.7 model.

6.3.4. Continental collisions

Collisions at continent-continent boundaries embodying fragments of Paleo- to Eoarchean protocrust (>3.2 Ga) led to the formation of old continental margins with very old high-μ or low-μ segments

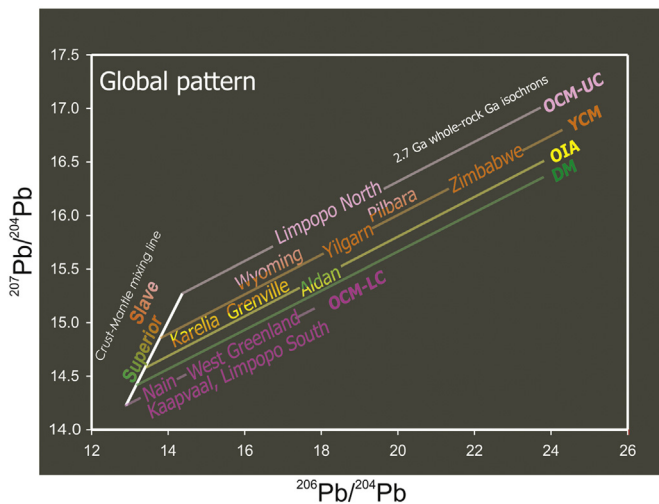


Fig. 15. A summary graph of Pb isotope ratios of 2.7 Ga whole-rock granitoids from different cratons on the RM 2.7 diagram. See Fig. 9 for acronyms. Data and references in Supplementary Table, individual plots in Halla (2014).

carrying very high-radiogenic or low-radiogenic signatures, respectively. Continental collisions probably exposed these contrasting lead sources for recycling.

The high-radiogenic end of the Slave Array and the previously mentioned Limpopo northern zone represent the most radiogenic compositions. Pb isotope compositions of K-feldspars plot close to the OCM-UC or OCM-LC signatures and whole-rock isochrons plot respectively close and parallel to the OCM-UC or -LC model lines.

In addition to previously mentioned Kaapvaal and Limpopo southern marginal zone, data from *West Greenland* (Taylor et al., 1980) and *Nain Province, Labrador* (Schjøtte et al., 1993) indicate the presence of >3.2 Ga low- μ crust. This is consistent with the Eoarchaeon ages up to 3.8 Ga obtained from the North Atlantic craton.

6.3.5. Correlating ancient continental margins

The RM 2.7 diagram indicates that the radiogenic Pb isotope characteristics of the mantle sources of granitoids correlates well with the age of the host cratons, suggesting that Pb isotopes of granitoids are useful in identifying and correlating the types of ancient convergent plate boundaries.

This pattern suggests that late Archaean granitoid magmas, formed at continental margins that encompass fragments of Early Archaean protocrust, inherited their high- μ or low- μ signatures from the protocrust by recycling through mantle. Thus, the Pb isotope systematics of Neoarchaeon granitoids reveal the age of the continental margin at which they were formed and the increasing crust-mantle interactions during the assembly of Neoarchaeon supercraton(s). Consequently, the Pb isotopes can be a powerful tool for craton correlations.

6.3.6. Granitoids and the growth of continents

According to the current knowledge, the evolution of continental crust started soon after the formation of the Earth with rather unknown Hadean basaltic crust (4.5–4.0 Ga). After the formation of the first known felsic rocks, the Acasta gneisses in the Slave Province, a long-term episodic TTG (tonalite-trondhjemite-granodiorite) magmatism of oceanic origin continued to be the major rock forming process until around 2.7 Ga.

At 3.0–2.5 Ga, geochemical diversification and the formation of multi-source diorite-granodiorite-granite batholiths indicated the appearance of convergent continental margins and collision zones (see a review of Halla et al., 2017, and references therein). The geochemical change in granitoids suggests a significant change in mantle dynamics and plate tectonics during the Neoarchaeon.

The global pattern on the RM 2.7 diagram suggests increasing crust-mantle interactions and development of continental-type convergent margins during an assembly of a Neoarchaeon supercraton, thus supporting the change observed in the geochemistry of granitoids.

6.4. A case study from West Karelia Province, eastern Finland

As an example of assessing tectonothermal effects and crustal contribution in the lead isotope compositions of individual granitoids, Figs. 16 and 17 plot Pb isotope data of K-feldspars and whole rocks of the Koitere and Nilsjö granitoid intrusions in the western margin of the Karelia craton, eastern Finland (Halla, 2005).

The plotted rocks are sanukitoid granodiorites that show clear geochemical mantle signatures; relatively low SiO₂, elevated Mg, Cr and Ni, high K-Ba-Sr-P signature typical of sanukitoids, and mafic magmatic enclaves (Heilimo et al., 2010). Their Hf, Nd, Pb, and O isotope results support a mantle source with a well-mixed crustal component (Heilimo et al., 2013). The single grain U–Pb zircon ages are similar, Koitere 2722 ± 6 Ga and Nilsjö 2724 ± 28 Ga, although the granitoids intrude different terrains (Heilimo et al., 2012).

The K-feldspars of the granitoids show variable deformation from undeformed orthoclase megacrysts (Fig. 16a) of orthopyroxene-bearing

granulite-facies portions of the Koitere granitoids to augen gneisses (Fig. 16b) with amphibolite-facies retrograde mineralogy (Halla and Heilimo, 2009).

The least radiogenic Pb isotope compositions of the Koitere undeformed orthoclase megacrysts plot on the model 2.7 Ga crust-mantle mixing line in Fig. 16c, suggesting that they have retained their initial compositions since crystallization. The deformed K-feldspars have not retained their initial Pb isotope compositions; they plot on secondary isochrons with an approximate slope of 1.9 Ga indicating redistribution of lead during Paleoproterozoic deformation.

The Koitere whole rocks plot approximately on the reference isochron of 2.73 Ga. The data plots close to the initial composition, indicating that the rock has lost most of its uranium at the time of its formation. The deformed K-feldspars plot on the reference secondary isochron at 1.9 Ga. The plots indicate that the Koitere granodiorites experienced a high-grade metamorphism soon after crystallization at 2.7 Ga and retrograde metamorphism at 1.9 Ga.

The Nilsjö granodiorites plot on a reference isochron with a slightly deeper slope. This may be due to a time gap between crystallization and metamorphism, which generated a transposed paleoisochron and transposed secondary K-feldspar isochron as explained in Fig. 6. However, the initial compositions for the Nilsjö granodiorites can be approximated from the diagram. Fig. 16c shows that the Nilsjö granitoids plot closer to the mantle value of Zartman and Doe (1981) than the Koitere granitoids. This is consistent with the Nd isotope results indicating contribution from older crust for the Koitere granitoids (Halla, 2005).

The interpretation of the Koitere and Nilsjö isochron slopes is consistent with younger granulite-facies metamorphic ages suggested for the Nilsjö (2.63 Ga from nearby granulites) than the Koitere (2.69 Ga from monazite) granodiorites.

The whole-rock data plot close to the initial compositions in Fig. 16, indicating that the U/Pb ratio of the rock has been low since its formation. The high Th/U trend in Fig. 17 supports the enrichment in Th with respect to U approximately at the time of formation. However, they originated in a source with an average Th/U ratio. This shows that the low-U content is a characteristic of the rock, not inherited from the source. Pb isotopes confirm that also rocks with retrograde mineralogy were metamorphosed at high-grade conditions. The Grenville data (Dickin, 1998; Gariépy et al., 1990), plotted for comparison in Fig. 17, show remarkably similar Pb isotope compositions.

In the RM 2.7 diagram (Fig. 15), the data from Koitere and Nilsjö plots on the DM-YCM field indicating a young continental margin setting for the Karelian granitoids. This is consistent with the known age range of the craton, 2.83–2.66 Ga with minor 3.2 Ga fragments.

In summary, Pb isotope compositions of the Nilsjö and Koitere granitoids indicate that the rocks crystallized at 2.73 Ga at a young continental margin setting, underwent high-grade metamorphism at the time of crystallization (Koitere) or 100 Ma later (Nilsjö), and experienced low-grade retrograde metamorphism at 1.9 Ga.

These results from eastern Finland show that interpretation of Pb isotope compositions in geological context can give much knowledge on the evolution of granitoids. The undeformed orthoclase megacrysts preserved their initial isotope composition, whereas K-feldspars with low-grade deformation microstructures registered and preserved the composition formed by redistribution of lead during Paleoproterozoic retrograde metamorphism. Low uranium and high thorogenic lead characteristics of the rock point to high-grade metamorphism relatively soon after crystallization. The Pb isotope data from the eastern margin of the Karelia craton show correlation with data from the Superior and, especially, from the Neoarchaeon parts of the Grenville province.

6.5. Concluding remarks

Pb isotope systematics of Archaean granitoids is a powerful tool in the studies of Archaean granite petrology and plate tectonics and can

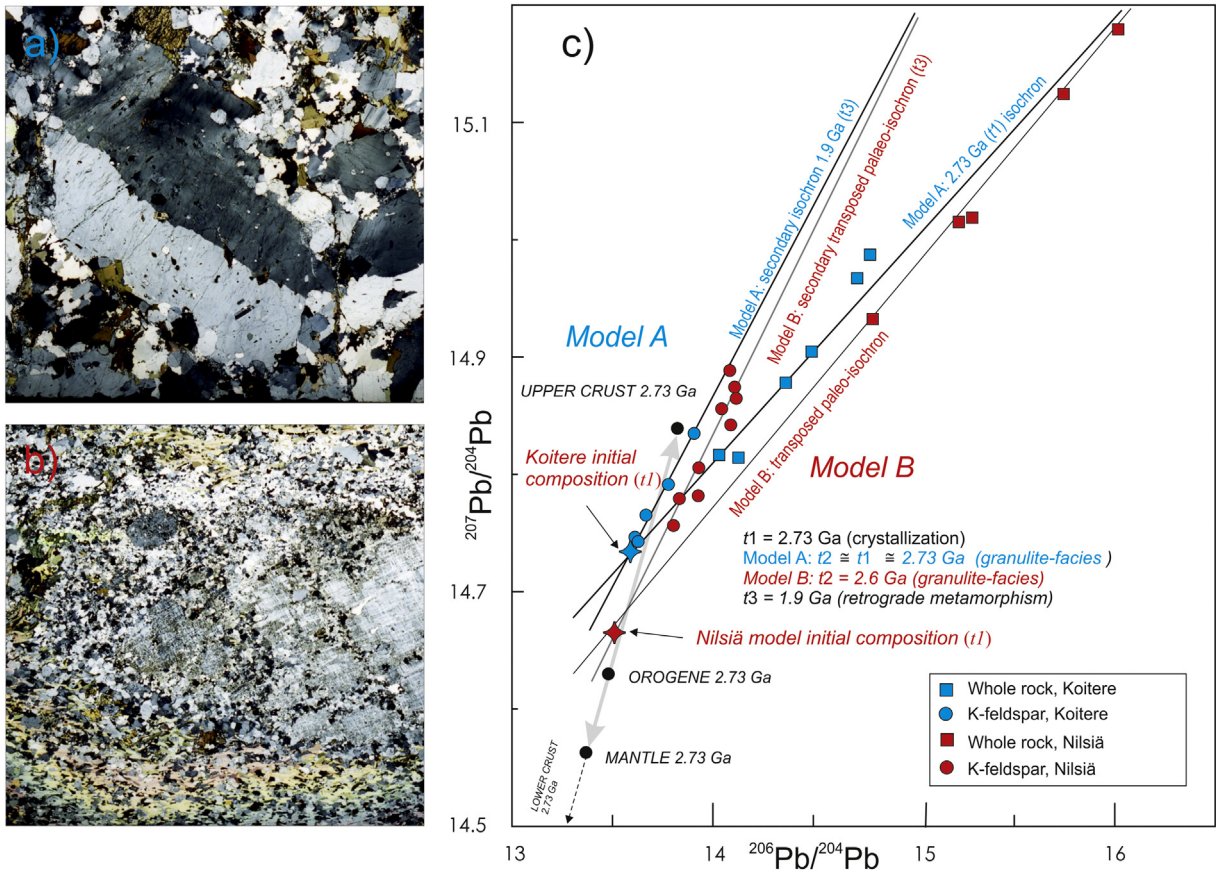


Fig. 16. Pb isotope data of K-feldspars and whole rocks from Koitere and Nilsjä granitoids from the Karelian Province, eastern Finland plotted on a $^{207}\text{Pb}/^{204}\text{Pb}$ - $^{206}\text{Pb}/^{204}\text{Pb}$ diagram. Model A and B isochrons (Fig. 6) are plotted for reference. The Nilsjä plot (Model B) is slightly transposed from the 2.7 and 1.9 isochrons of Model A indicating a longer gap between crystallization and metamorphism. The Koitere data plots on the Model A. Model initial Pb isotope compositions on the crust-mantle mixing line from Zartman and Doe (1981).

contribute many research questions on petrogenesis and tectonothermal evolution of granitoids, crust-mantle recycling at convergent continental margins, identification of ancient collision zones, and correlating Archaean supercratons.

Pb isotope systematics within a whole-rock granitoid can reveal both low- and high-grade tectonothermal events after crystallization, which is based on the formation of secondary K-feldspar isochrons and paleoisochrons, respectively.

Tracing initial Pb/Pb isotope ratios by analysing K-feldspars or diagrams can give information on contributions from older crust; the higher the ^{207}Pb ratio with respect to ^{206}Pb , the older the continental margin from which crustal lead was extracted and recycled to the mantle. Because Pb isotope composition of granitoids holds traces of the accretionary history of the host province, oceanic-oceanic, oceanic-continent and old continent-continent plate boundaries have distinct mantle isotope compositions.

By mapping the relative amount of ^{207}Pb across wide areas, it is possible to trace allochthonous terrains and correlate similar terrains in different parts of the world. Correlation of mantle keels with distinct isotope compositions that reflect the evolution of the overlying craton is directly applicable in supercontinent correlations. Furthermore, detecting high Th/U trends helps in identifying zones of Neoproterozoic continental collisions and high-grade metamorphic belts.

Time-fixed Pb isotope model for 2.7 Ga mantle-derived granitoids show a global pattern that probably reflects accretion of island arcs to protocontinents and continental collisions, pointing to Neoproterozoic subduction and supercontinent formation. The benefit of the model is that it can be used as a tectonic discriminating diagram without full knowledge on the complex methodological background, but it is also possible to recalculate the model to represent any other important peak of crustal growth. It is also possible to add multiple stages in the model by calculating Pb/Pb ratios at selected time points backward from the present.

Pb isotope systematics of granitoids, when interpreted in the context of chronological, petrological, geochemical and other isotope data, are a powerful tool for resolving questions on Archaean continental growth from large-scale tectonics to the magmatic and tectonothermal history of individual intrusions.

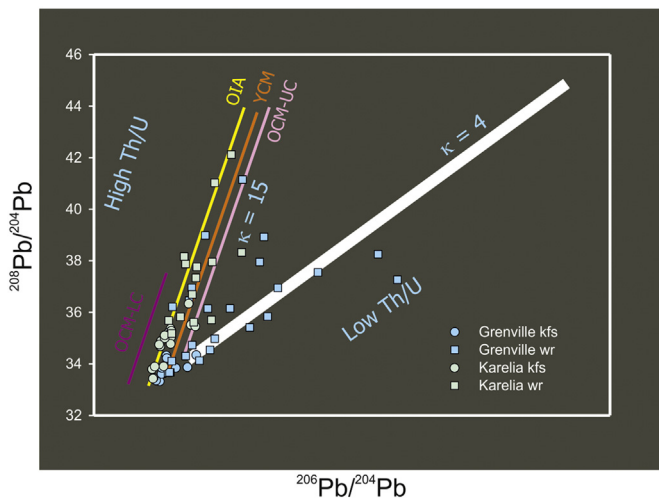


Fig. 17. The Nilsjä and Koitere data from the Karelian province plotted on the $^{207}\text{Pb}/^{204}\text{Pb}$ - $^{206}\text{Pb}/^{204}\text{Pb}$ diagram with the RM 2.7 model lines calculated for $\kappa = 15$ and $\kappa = 4$. Data from the Grenville province is plotted for comparison.

Acknowledgements

Reviewers Tom Andersen and Pat Castillo are greatly acknowledged and appreciated for their excellent and constructive comments on the manuscript. This work was inspired by the IGCP-SIDA 599 Project ‘The Changing Early Earth’ (2011–2015) sponsored by UNESCO and SIDA and by the support from the K.H. Renlund Foundation, Finland, Academy of Finland, DST (Department of Science and Technology), India, and Finnish Museum of Natural History. I would like to thank the participants of the IGCP-SIDA 599 project for the lively and enthusiastic discussions during meetings and field trips.

Appendix A. Equations describing the evolution of lead

The change in the isotopic composition of lead relative to the stable index isotope ^{204}Pb in a U-bearing system of age T (starting time of the system) that has remained closed to uranium and lead until the time t of separation of Pb from U (ending time of the system) can be described by the following equation:

$$\left(\frac{^{206}\text{Pb}}{^{204}\text{Pb}}\right)_t = \left(\frac{^{206}\text{Pb}}{^{204}\text{Pb}}\right)_T + \mu(e^{\lambda_{238}T} - e^{\lambda_{238}t}) \quad (1)$$

where λ_{238} is the decay constant of ^{238}U , μ is the term referred to as the milieu index describing the present-day $^{238}\text{U}/^{204}\text{Pb}$ ratio of the source, and

$$\begin{aligned} \left(\frac{^{206}\text{Pb}}{^{204}\text{Pb}}\right)_t &= \text{isotope ratio of Pb of age } t, \text{ and} \\ \left(\frac{^{206}\text{Pb}}{^{204}\text{Pb}}\right)_T &= \text{isotope ratio of Pb of age } T. \end{aligned}$$

If $t = 0$, Eq. (1) reduces to

$$\left(\frac{^{206}\text{Pb}}{^{204}\text{Pb}}\right)_t = \left(\frac{^{206}\text{Pb}}{^{204}\text{Pb}}\right)_T + \mu(e^{\lambda_{238}T} - 1). \quad (2)$$

Similar equations can be written for the two other decay schemes:

$$\left(\frac{^{207}\text{Pb}}{^{204}\text{Pb}}\right)_t = \left(\frac{^{207}\text{Pb}}{^{204}\text{Pb}}\right)_T + \frac{\mu}{137.88}(e^{\lambda_{235}T} - e^{\lambda_{235}t}) \quad (3)$$

and

$$\left(\frac{^{208}\text{Pb}}{^{204}\text{Pb}}\right)_t = \left(\frac{^{208}\text{Pb}}{^{204}\text{Pb}}\right)_T + \omega(e^{\lambda_{232}T} - e^{\lambda_{232}t}). \quad (4)$$

where λ_{235} is the decay constant of ^{235}U , λ_{232} is the decay constant of ^{232}Th , and ω is the milieu index describing the present-day $^{232}\text{Th}/^{204}\text{Pb}$ ratio of the source.

If $t = 0$, Eq. (4) reduces to

$$\left(\frac{^{208}\text{Pb}}{^{204}\text{Pb}}\right)_t = \left(\frac{^{208}\text{Pb}}{^{204}\text{Pb}}\right)_T + \omega(e^{\lambda_{232}T} - 1). \quad (5)$$

The evolution of lead can be described on a $^{207}\text{Pb}/^{204}\text{Pb}$ vs. $^{206}\text{Pb}/^{204}\text{Pb}$ or $^{208}\text{Pb}/^{204}\text{Pb}$ vs. $^{206}\text{Pb}/^{204}\text{Pb}$ diagram in terms of *growth curves*, based on Eqs. (1) and (3) or (1) and (4). A growth curve originates at the point representing the isotope composition of the primordial lead. Each growth curve represents the change in lead isotope ratios over time for a system with a particular value of μ or ω .

Eqs. (1) and (3) may be combined and μ eliminated because the $^{235}\text{U}/^{238}\text{U}$ ratio is known to be constant, equal to 1/137.88 for all U of

normal isotopic composition in the Earth at the present time.

$$\frac{\left(\frac{^{207}\text{Pb}}{^{204}\text{Pb}}\right)_t - \left(\frac{^{207}\text{Pb}}{^{204}\text{Pb}}\right)_T}{\left(\frac{^{206}\text{Pb}}{^{204}\text{Pb}}\right)_t - \left(\frac{^{206}\text{Pb}}{^{204}\text{Pb}}\right)_T} = \frac{1}{137.88} \frac{[e^{\lambda_{235}T} - e^{\lambda_{235}t}]}{[e^{\lambda_{238}T} - e^{\lambda_{238}t}]} \quad (6)$$

When the values of t are constant, a family of straight lines is formed on a $^{207}\text{Pb}/^{204}\text{Pb}$ vs. $^{206}\text{Pb}/^{204}\text{Pb}$ diagram according to Eq. (6). These straight lines, each corresponding to a particular value of t , are termed *isochrons*. All the isochrons pass through a common point representing the primordial lead isotope ratio (Fig. 1). The slope of a given isochron depends only on times T and t . The slope of the isochron can be calculated by the equation.

$$m = \frac{1}{137.88} \frac{[e^{\lambda_{235}T} - e^{\lambda_{235}t}]}{[e^{\lambda_{238}T} - e^{\lambda_{238}t}]} \quad (7)$$

This transcendental equation cannot be solved for an age by conventional algebraic methods, but it can be solved by a graphical method, by means of table giving the slopes of the isochrons as a function of t , or by computer.

If $t = 0$, Eq. (7) reduces to

$$m = \frac{1}{137.88} \frac{[e^{\lambda_{235}T} - 1]}{[e^{\lambda_{238}T} - 1]} \quad (8)$$

Appendix A. Supplementary data

Supplementary data to this article can be found online at <https://doi.org/10.1016/j.lithos.2018.08.031>.

References

- Aston, F.W., 1919. LXXIV. A positive ray spectrograph. The London, Edinburgh, and Dublin Philosophical Magazine and Journal of Science 38, 707–714.
- Aston, F.W., 1927. The constitution of ordinary lead. Nature 120, 224.
- Ayer, J.A., Dostal, J., 2000. Nd and Pb isotopes from the Lake of the Woods greenstone belt, northwestern Ontario: implications for mantle evolution and the formation of crust in the southern Superior Province. Canadian Journal of Earth Sciences 37, 1677–1689.
- Barton, J.M., Doig, R., Smith, C.B., Bohlender, F., van Reenen, D.D., 1992. Isotopic and REE characteristics of the intrusive charnoenderbite and enderbite geographically associated with the Matok pluton, Limpopo Belt, southern Africa. Precambrian Research 55, 451–467.
- Berger, M., Rollinson, H., 1997. Isotopic and geochemical evidence for crust–mantle interaction during late Archean crustal growth. Geochimica et Cosmochimica Acta 61, 4809–4829.
- Bickle, M.J., Chapman, H.J., Bettenay, L.F., Groves, D.I., de Laeter, J.R., 1983. Lead ages, reset rubidium–strontium ages and implications for the Archean crustal evolution of the Diemals area, Central Yilgarn Block, Western Australia. Geochimica et Cosmochimica Acta 47, 907–914.
- Bleeker, W., 2003. The late Archean record: a puzzle in ca. 35 pieces. Lithos 71, 99–134.
- Carignan, J., Gariépy, N., Machado, N., Rive, M., 1993. Pb isotopic geochemistry of granitoids and gneisses from the late Archean Pontiac and Abitibi Subprovinces of Canada. Chemical Geology 106, 299–316.
- Carignan, J., Machado, N., Gariépy, C., 1995. Initial Pb isotope composition of silicate minerals from the Mulcahy layered intrusion: Implications for the nature of the Archean mantle and the evolution of greenstone belts in the Superior Province, Canada. Geochimica et Cosmochimica Acta 59, 97–105.
- Cumming, G.L., Richards, J.R., 1975. Ore lead in a continuously changing Earth. Earth and Planetary Science Letters 28, 155–171.
- Davis, W.J., Gariépy, C., van Breemen, O., 1996. Pb isotope composition of late Archean granites and the extent of recycling early Archean crust in the Slave Province, Northwest Canada. Chemical Geology 130, 255–269.
- Davis, D.W., Williams, I.S., Krogh, T.E., 2003. Historical Development on Zircon Geochronology. Reviews in Mineralogy and Geochemistry 53, 145–181.
- Dempster, A.J., 1917. A new method of positive ray analysis. Physical Review Journals 11, 316–325.
- Dickin, A.P., 1998. Pb isotope mapping of differentially uplifted Archean basement: a case study from the Grenville Province, Ontario. Precambrian Research 91, 445–454.
- Doe, B.R., Rohrbough, R., 1977. Lead Isotope Data Bank; 3,458 Samples and analyses cited. U.S. Geological Survey Open-File Report 79 (274).
- Doe, B.R., Zartman, R.E., 1979. Plumbotectonics, the Phanerozoic. In: Barnes, H.L. (Ed.), Geochemistry of Hydrothermal Ore Deposits 22–70, 2nd edition John Wiley & Sons, New York.

- Dostal, J., Capedri, S., 1975. Partition coefficients of uranium for some rock-forming minerals. *Chemical Geology* 15, 285–294.
- Gale, N.H., Mussett, A.E., 1973. Episodic Uranium-Lead Models and the Interpretation of Variations in the Isotopic Composition of Lead in Rocks. *Reviews of Geophysics and Space Physics* 11, 37–86.
- Gancarz, A.J., Wasserburg, G.J., 1977. Initial Pb of the Amitsoq gneiss, West Greenland and implications for the age of the Earth. *Geochimica Cosmochimica Acta* 41, 1283–1301.
- Gariépy, C., Allégre, J., 1985. The lead isotope geochemistry and geochronology of late-kinematic intrusives from the Abitibi greenstone belt, and the implications for late Archean crustal evolution. *Geochimica et Cosmochimica Acta* 49, 2371–2383.
- Gariépy, C., Verner, D., Doig, R., 1990. Dating Archean metamorphic minerals southeast of the Grenville front, western Quebec, using Pb isotopes. *Geology* 18, 1078–1081.
- Griffin, W.L., Taylor, P.N., Hakkinea, J.W., Heier, K.S., Idea, I.K., Krogh, E.J., Malm, O., Olsen, K.I., Ormaasen, D.E., Treten, E., 1978. Archean and Proterozoic crustal evolution in Lofoten-Vesterålen, Norway. *Journal of the Geological Society of London* 135, 629–647.
- Halla, J., 2005. Late Archean high-Mg granitoids (sanukitoids) in the southern Karelian Domain, eastern Finland: Pb and Nd isotope constraints on crust-mantle interactions. *Lithos* 79, 161–178.
- Halla, J., 2014. Recycling of Lead at Neoproterozoic Continental Margins. In: Dilek, Y., Furnes, H. (Eds.), *Evolution of Archean Crust and Early Life. Modern Approaches in Solid Earth Sciences*. Vol. 7. Springer, Berlin, pp. 195–214.
- Halla, J., Heilimo, E., 2009. Deformation-induced Pb isotope exchange between K-feldspar and whole rock in Neoproterozoic granitoids: Implications for assessing Proterozoic imprints. *Chemical Geology* 265, 303–312.
- Halla, J., van Hunen, J., Heilimo, E., Hölttä, P., 2009. Geochemical and numerical constraints on Neoproterozoic plate tectonics. *Precambrian Research* 174, 155–162.
- Halla, J., Whitehouse, M.J., Ahmad, T., Bagai, Z., 2017. Archean granitoids: an overview and significance from a tectonic perspective. In: Halla, J., Whitehouse, M.J., Ahmad, T. & Bagai, Z. (eds) *Crust–Mantle Interactions and Granitoid Diversification: Insights from Archean Cratons*. Geological Society, London, Special Publications 449, 1–18.
- Heilimo, E., Halla, J., Hölttä, P., 2010. Discrimination and origin of the sanukitoid series: geochemical constraints from the Neoproterozoic western Karelia Province (Finland). *Lithos* 115, 27–39.
- Heilimo, E., Halla, J., Andersen, T., Huhma, H., 2012. Neoproterozoic Crustal Recycling and Mantle Metasomatism: Hf–Nd–Pb–O Isotope Evidence from Sanukitoids of the Fennoscandian Shield.
- Heilimo, E., Halla, J., Andersen, T., Huhma, H., 2013. Neoproterozoic crustal recycling and mantle metasomatism: Hf–Nd–Pb–O isotope evidence from sanukitoids of the Fennoscandian Shield. *Precambrian Research* 228, 250–266.
- Henry, P., Stevenson, R.K., Gariépy, C., 1998. Late Archean mantle composition and crustal growth in the Western Superior Province of Canada: Neodymium and lead isotopic evidence from the Wawa, Quetico, and Wabigoon subprovinces. *Geochimica et Cosmochimica Acta* 62, 143–157.
- Holmes, A., 1946. An estimate of the age of the earth. *Nature* 157, 680–684.
- Houtermans, F.G., 1946. Die Isotopenhäufigkeiten im natürlichen Blei und da Alter des Urans. *Naturwissenschaften* 33, 185–186, 219.
- Isnard, H., Gariépy, C., 2004. Sm–Nd, Lu–Hf and Pb–Pb signatures of gneisses and granitoids from the La Grande belt: Extent of Archean crustal recycling in the northeastern Superior Province, Canada. *Geochimica et Cosmochimica Acta* 68, 1099–1113.
- Jelsma, H.A., Vinyu, M.L., Valbracht, P.J., Davies, G.R., Wijbrans, J.R., Verdurmen, E.A.T., 1996. Constraints on Archean crustal evolution of the Zimbabwe craton: a U–Pb zircon, Sm–Nd and Pb–Pb whole-rock isotopic study. *Contributions to Mineralogy and Petrology* 124, 55–70.
- Kamber, B.S., Collerson, K.D., Moorbath, S., Whitehouse, M.J., 2003. Inheritance of early Archean Pb-isotope variability from long-lived Hadean protocrust. *Contributions to Mineralogy and Petrology* 145, 25–46.
- Kanasewich, E.R., 1968. The Interpretation of Lead Isotopes and their Geological Significance. In: Hamilton, I., Farquhar, R.M. (Eds.), *Radiometric Dating for Geologists*. Wiley, Interscience, New York, pp. 147–223.
- Kramers, J.D., Tolstikhin, I.N., 1997. Two terrestrial lead isotope paradoxes, forward transport modelling, core formation and the history of the continental crust. *Chemical Geology* 139, 75–110.
- Kreissig, K., Nägler, T.F., Kramers, J.D., van Reenen, D.D., Smit, C.A., 2000. An isotopic and geochemical study of the northern Kaapvaal Craton and the Southern marginal Zone of the Limpopo Belt: are they juxtaposed terranes? *Lithos* 50, 1–25.
- McNaughton, N.J., Bickle, M.J., 1987. K-feldspar Pb–Pb isotope systematics Archean post-kinematic granitoid intrusions of the Diemals area, central Yilgarn Block, Western Australia. *Chemical Geology (Isotope Geoscience Section)* 66, 193–208.
- Moorbath, S., Taylor, P.N., 1981. Isotopic evidence for continental growth in the Precambrian. In: Kröner, A. (Ed.), *Precambrian Plate Tectonics*. Elsevier, Amsterdam, pp. 491–525.
- Neymark, L.A., Kovach, V.P., Nemchin, A.A., Morozova, I.M., Kotov, A.B., Vinogradov, D.P., Gorokhovskiy, B.M., Ovchinnikova, G.V., Bogomolova, L.M., Smelov, A.P., 1993. Late Archean intrusive complexes in the Olekma granite-greenstone terrain (eastern Siberia): geochemical and isotope study. *Precambrian Research* 62, 453–472.
- Nier, A.O., 1938. Variations in the relative abundances of the isotopes of common lead from various sources. *Journal of American Chemical Society* 60, 1571–1576.
- Oversby, V.M., 1975. Lead isotopic systematics and ages of Archean acid intrusives in the Kalgoorlie–Norseman area, Western Australia. *Geochimica et Cosmochimica Acta* 39, 1107–1125.
- Patterson, C., 1956. Age of meteorites and the Earth. *Geochimica Cosmochimica Acta* 10, 230–237.
- Rosholt, J.N., Zartman, R.E., Nkomo, I.T., 1973. Pb isotope systematics and uranium depletion in the Granite Mountains, Wyoming. *Geological Society of America Bulletin* 84, 989–1002.
- Russell, R.D., Farquhar, R.M., 1960. *Lead Isotopes in Geology*. Vol. 243. Wiley Interscience, New York.
- Schiøtte, L., Hansen, B.T., Shirey, S.B., Bridgwater, D., 1993. Petrological and whole rock isotopic characteristics of tectonically juxtaposed Archean gneisses in the Okak area of the Nain Province, Labrador: relevance for terrane models. *Precambrian Research* 63, 293–323.
- Stacey, J.S., Kramers, J.D., 1975. Approximation of terrestrial lead isotope evolution by a two-stage model. *Earth and Planetary Science Letters* 26, 207–221.
- Stevenson, R., Henry, P., Gariépy, C., 1999. Assimilation-fractional crystallization origin of Archean Sanukitoid Suites: Western Superior Province, Canada. *Precambrian Research* 96, 83–99.
- Taylor, P.N., Moorbath, S., Goodwin, R., Petrykowski, A.C., 1980. Crustal contamination as an indicator of the extent of early Archean continental crust: Pb isotopic evidence from the late Archean gneisses of West Greenland. *Geochimica et Cosmochimica Acta* 44, 1437–1453.
- Whitehouse, M.J., 1989. Pb-isotopic evidence for U–Th–Pb behaviour in a prograde amphibolite to granulite facies transition from the Lewisian complex of north-West Scotland: Implications for Pb–Pb dating. *Geochimica et Cosmochimica Acta* 53, 717–724.
- Wooden, J.L., Mueller, P.A., 1988. Pb, Sr, and Nd isotopic compositions of a suite of late Archean, igneous rocks, eastern Beartooth Mountains: implications for crust–mantle evolution. *Earth and Planetary Science Letters* 87, 59–72.
- Yamashita, K., Creaser, R.A., Stemler, J.U., Zimaro, T.W., 1999. Geochemical and Nd–Pb isotopic systematics of late Archean granitoids, southwestern Slave Province, Canada: constraints for granitoid origin and crustal isotopic structure. *Canadian Journal of Earth Sciences* 36, 1131–1147.
- Zartman, R.E., 1965. The isotopic composition of lead in microclines from the Llano uplift, Texas. *Journal of Geophysical Research* 70, 965–975.
- Zartman, R.E., Doe, B.R., 1981. Plumbotectonics - the model. *Tectonophysics* 75, 135–162.
- Zartman, R.E., Haines, S.M., 1988. The plumbotectonic model for Pb isotopic systematics among major terrestrial reservoirs - a case for bi-directional transport. *Geochimica et Cosmochimica Acta* 52, 1327–1339.